

# Novel Synthesis of Cerium Hexaboride by Hexamine Route

K. Amalajyothi<sup>a</sup> and L. J. Berchmans<sup>b</sup>

<sup>a</sup> Department of Electrochemical Engineering, Center for Education, Central Electrochemical Research Institute, Karaikudi, Tamil Nadu, 630006 India

<sup>b</sup> Electropyrometallurgy Division, Central Electrochemical Research Institute, Karaikudi, Tamil Nadu, 630006 India

e-mail: ljberchmans@yahoo.com

Received September 8, 2008

**Abstract**—An endeavor has been made to prepare cerium hexaboride using a mixture of cerium nitrate, boron trioxide, and hexamine as a fuel burning at a relatively low temperature (500°C). The product was characterized by X-ray diffraction (XRD), FT-IR, TGA/DTA, SEM, and TEM. The upshot of the exploration exemplifies that CeB<sub>6</sub> with a crystallite size of about 50 nm can be beneficially prepared. Some impurities are also perceived with the pure compound, which embodies the presence of lower valence cerium borides.

**Keywords:** chemical synthesis, XRD, FT-IR, SEM, TEM.

PACS numbers: 81.05.Mh, 81.16.Be, 81.20.Ka

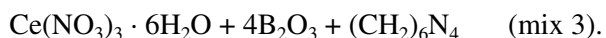
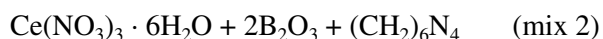
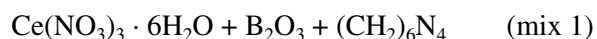
DOI: 10.3103/S106138620804002X

## 1. INTRODUCTION

Rare-earth hexaborides RB<sub>6</sub> epitomize far-fetched properties such as highly efficient thermionic emission [1, 2] superconductivity [3–5], narrow-band semiconductivity [6], magnetic ordering [7], high melting temperature, strength and chemical stability [8, 9] because of the electron paucity of boron [10]. Among these, cerium hexaboride CeB<sub>6</sub> finds application in many advanced fields. It has a very low work function (around 2.5 eV), low volatility, and longer service life [11, 12]. It is used in electronic devices, decorative coatings [13, 14], and nuclear technology [15] because of its high thermal neutron cross section of <sup>10</sup>B [16]. Boron-rich rare-earth borides can be prepared by molten salt electrolysis [17], solution method [18], and floating zone method [19–21]. In the above methods, the reaction temperature is above 1000°C and processing is time-consuming. In this work, we made an attempt to synthesize cerium hexaboride crystals in a low-temperature process using hexamine as a fuel.

## 2. EXPERIMENTAL

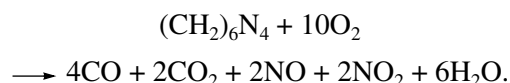
Cerium nitrate Ce(NO<sub>3</sub>)<sub>3</sub> · 6H<sub>2</sub>O, boron trioxide B<sub>2</sub>O<sub>3</sub>, and hexamine (CH<sub>2</sub>)<sub>6</sub>N<sub>4</sub> were mixed in the following stoichiometric proportions:



Mixtures (1)–(3) were placed in a high alumina crucible and put into an inconel reactor which had the inlet/outlet for argon gas. Then the reactor was heated in an electric furnace to 500°C. The intact experiments were carried out in a controlled argon atmosphere for 10 h. After completion of the reaction, the contents were detached from the crucible and treated with dilute HCl followed by washing with triple distilled water. Then the product is washed with ethanol and desiccated at 150°C in an oven. The purified product was characterized by XRD (Philips 8030 X-Ray Diffractometer) to identify the phase composition. The particle size distribution of the powders was analyzed using a particle size analyzer Microtrac S3500. The morphology of the synthesized crystals was scrutinized by SEM (JEOL-JSM-3.5 CF-Japan) and TEM (FEI Technai 20 G<sup>2</sup>).

## 3. RESULTS AND DISCUSSION

Hexamine—also called hexamethylenetetramine (HMT), or methenamine—is a heterocyclic organic compound widely used in organic synthesis [22]. The combustion reaction of hexamine can be represented as



Hexamine was tried as a fuel for preparation of LiMn<sub>2</sub>O<sub>4</sub> nanoparticles [23], alumina nanofibers [24], zinc oxide [25, 26], MgAl<sub>2</sub>O<sub>4</sub>, ZnAl<sub>2</sub>O<sub>4</sub> [27], dispersed bimetallic carbides and nitrides [28–30], and alumina-supported g-Mo<sub>2</sub>N [31]. One of the simplest and most promising methods is single-step decomposition of a

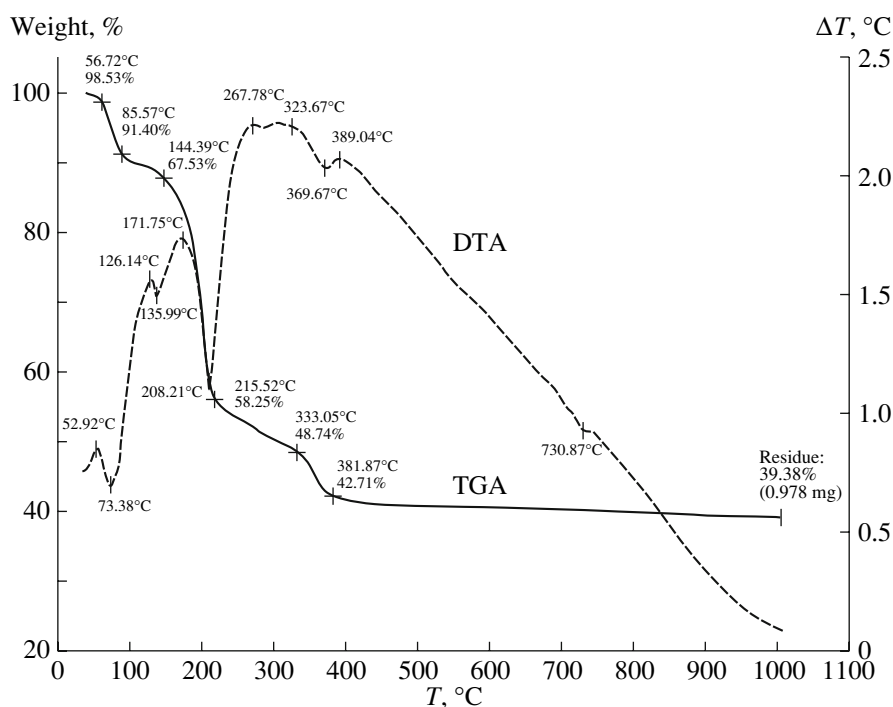


Fig. 1. TGA/DTA curves for mix 1.

HMT-based complex [32]. Afanasiev [32] has reported the synthesis of high surface area  $\text{Mo}_2\text{N}$  by thermal decomposition of HMT complex at low temperature (823–1073 K). In our experiments, hexamine has been used to form a complex with the reactants subsequent decomposition of which yields cerium hexaboride  $\text{CeB}_6$ .

Figure 1 shows the TGA/DTA curves for mix 1. As follows from the TGA curve, the loss of crystallization water [from  $\text{Ce}(\text{NO}_3)_3 \cdot 6\text{H}_2\text{O}$ ] seen at 85.57°C attains its maximum value at 216.52°C, which is followed by chemical decomposition at 381.87°C. Beyond

381.87°C, there is no weight loss, which indicates that the resultant compound does not undergo any chemical change. It has been calculated that of the weight loss above 30% may be due to the removal of water and partial chemical decomposition of mixture. This information has been inferred from the TGA curve.

The DTA curve in Fig. 1 exhibits three dips corresponding to endothermic reactions: the dips at 73.38°C and 216.52°C can be associated with dehydration while that at 369.67°C, with decomposition of associated gas-

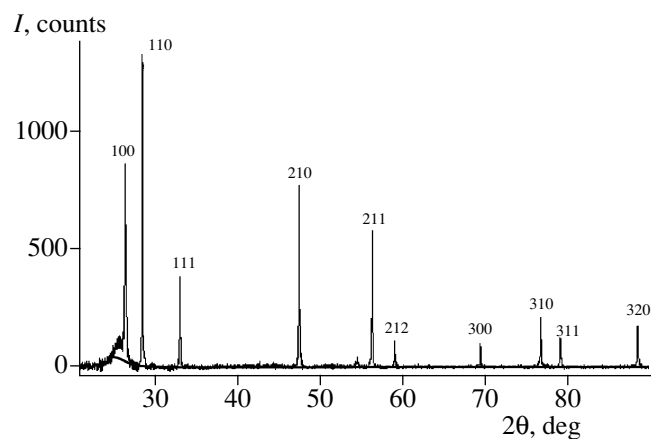


Fig. 2. XRD pattern of synthesized  $\text{CeB}_6$ .

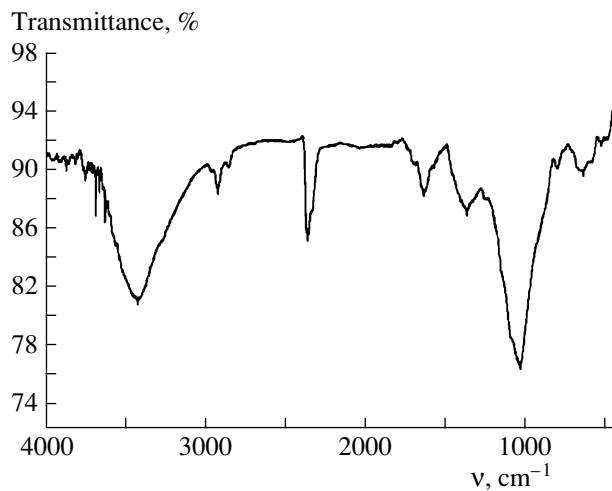


Fig. 3. FT-IR spectrum of synthesized  $\text{CeB}_6$ .

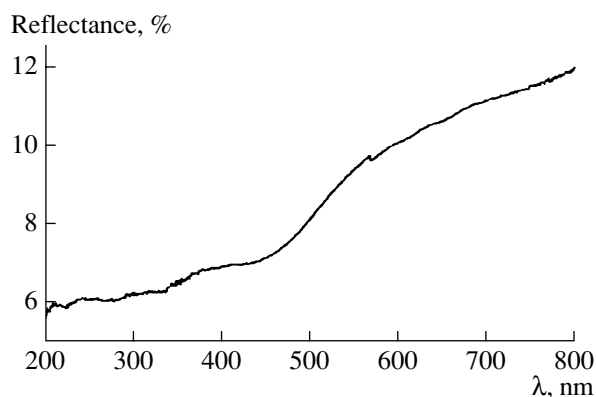


Fig. 4. The reflectance spectrum of synthesized  $\text{CeB}_6$ .

eous product, which is the minimum melting temperature of the compound. In the upstream side, an exothermic peak at  $323.67^\circ\text{C}$  is primarily due to the decomposition of hydrogen and oxygen, which is vital for melting the reactants to the recovered temperature of above  $369.67^\circ\text{C}$  and a good yield of cerium hexaboride.

The XRD pattern for the synthesized compound is shown in Fig. 2. The most of the peaks are seen to match the standard data. The XRD data were used to calculate the lattice constant  $a$  and the size of  $\text{CeB}_6$  crystallites (see Table 1). The calculated values of  $a$  are in good agreement with the published value for  $\text{CeB}_6$ :  $a = 4.14 \text{ \AA}$  (JCPDS data card no. 88-02072). The crystallite size was found to vary between 205 and 226 nm, depending on the composition of starting mixtures used in experiments.

The Fourier-transform IR (FT-IR) spectrum of synthesized  $\text{CeB}_6$  recorded over the range  $400\text{--}4000 \text{ cm}^{-1}$  (Fig. 3) exhibits the well-pronounced bands at  $1028.2 \text{ cm}^{-1}$ ,  $645.7 \text{ cm}^{-1}$ ,  $418.4 \text{ cm}^{-1}$  etc. attributed to the Ce–B bond [33], thus confirming the formation of single-phase crystalline cerium hexaboride.

Figure 4 shows the reflectance spectrum of synthesized  $\text{CeB}_6$ . Using this spectrum, we calculated the energy band gap by plotting the graph  $E \text{ (eV)}$  vs.  $\{\ln[h\nu(R_{\max} - R_{\min})/(R - R_{\min})]\}^2$ . Here  $R_{\max}$  and  $R_{\min}$  are the maximum and minimum reflectance in the reflectance spectrum, respectively, and  $R$  is the running

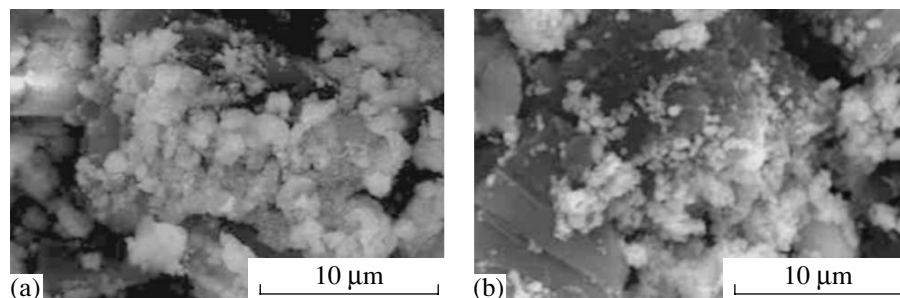


Fig. 5. SEM micrographs of the  $\text{CeB}_6$  obtained from (a) mix 2 and (b) mix 3.

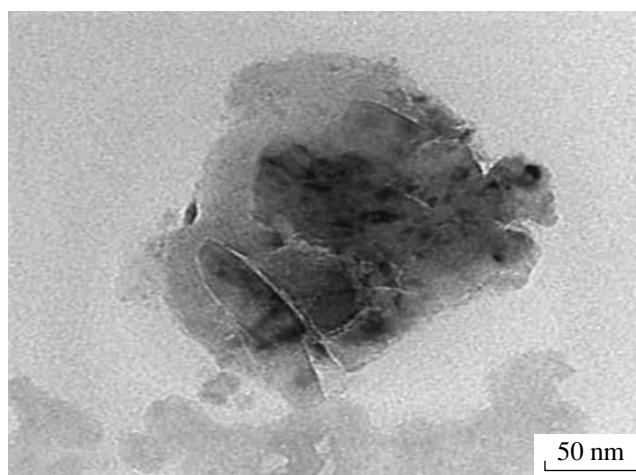


Fig. 6. High-resolution TEM image of  $\text{CeB}_6$  crystallite.

**Table 1.** Lattice constants ( $a$ ) and the size of  $\text{CeB}_6$  crystallites ( $d$ ) formed in mixtures 1–3

Starting mixture	$a$ , Å	$d$ , nm
Mix 1	4.1295	54
Mix 2	4.1365	52
Mix 3	4.1398	50

**Table 2.** Chemical analysis of impurity elements in the products obtained from mixtures 1–3

Starting mixture	N	C	S	H
Mix 1	3.126	13.265	0.923	2.262
Mix 2	2.674	12.674	0.813	1.562
Mix 3	1.785	10.012	0.050	0.050

energy of photons. The plot was found to be linear. Its extrapolation to  $\{\ln[h\nu(R_{\max} - R_{\min})/(R - R_{\min})]\}^2 = 0$  gave a value of the direct band gap equal approximately to 3.01 eV, which also confirms the formation of homogenous product in our experiments.

The data of chemical analysis (see Table 2) shows that the product obtained from mix 1 contains a higher amount of N- and C-containing impurities. With increasing amount of  $\text{B}_2\text{O}_3$  in starting mixtures (mixtures 2 and 3), the amount of N-, S-, H-containing impurities becomes negligibly small.

The SEM micrographs presented in Fig. 5 show that the product grains possess an irregular shape with a fine structure. With increasing boron content, the product morphology changes and exhibits a still finer spheroid grain structure.

Figure 6 shows the high-resolution TEM image of  $\text{CeB}_6$  crystallite. Typically, the  $\text{CeB}_6$  crystallites are around 50 nm in diameter and have a regular shape.

#### 4. CONCLUSIONS

Fine powders of crystalline  $\text{CeB}_6$  have been successfully synthesized at a relatively low temperature (500°C) using hexamine as a fuel.

#### REFERENCES

- Otani, S. and Ishizawa, Y., *J. Alloys Compd.*, 1996, vol. 245, pp. L18–L20.
- Laffery, A., *J. Appl. Phys.*, 1951, vol. 22, pp. 299–304.
- Schwarzkopf, P., Kieffer, R., Leszynski, W., and Benesorsky, K., *Refractory Hard Metals: Borides, Carbides, Nitrides, and Silicides*, New York: Macmillan, 1953.
- Hulm, J.K. and Matthias, B.T., *Phys. Rev.*, 1951, vol. 82, p. 273.
- Matthias, B.T. and Hulm, K.J., *Phys. Rev.*, 1952, vol. 87, p. 799.
- Bat'ko, I., Bat'kova, M., and Flachbart, K., *J. Alloys Compd.*, 1985, vol. 217, pp. L1–L3.
- Etuorneau, J. and Hagemuller, P., *Philos. Mag.*, 1985, vol. 52, p. 589.
- Eristavi, A., Kalandadze, G., Magalashvili, B., and Shalamberidze, S., *J. Mater. Process. Manuf. Sci.*, 1998, vol. 6, p. 239.
- Kiessling, R., *Acta. Chem. Scand.*, 1950, vol. 4, p. 209.
- Liu, Y., Lu, W.J., Qin, J.N., and Zhang, D., *J. Alloys Compd.*, 1997, vol. 431, pp. 337–341.
- Swanaon, L.W. and McNeely, D.R., *Surf. Sci.*, 1979, vol. 83, pp. 11–15.
- Davis, P.R., Gesley, M.A., Schwind, G.A., and Swanson, L.W., *Appl. Surf. Sci.*, 1989, vol. 37, pp. 381–385.
- Nakasuhi, M. and Wada, H., *J. Vac. Sci. Technol.*, 1980, vol. 17, p. 1367.
- Zega, B., *Surf. Coat. Technol.*, 1989, vols. 39–40, p. 507.
- Meschel, S.V. and Kleppa, O.J., *J. Alloys Compd.*, 1995, vol. 226, pp. 243–247.
- Bala Krishnan, G., Lees, M.R., and Daul, D.M.K., *J. Cryst. Growth*, 2003, vol. 256, pp. 206–209.
- Shen, P., Gong, Y., Zhou, Y., Lin, D., and Wuji, H., *Xuebao*, 1991, vol. 7, pp. 306–312.
- Gurin, V.V., Korsukova, M.M., Nikanorov, S.P., Smirnov, I.A., Stepanov, N.N., and Shul'man, S.G., *J. Less-Common Met.*, 1979, vol. 67, pp. 115–119.
- Tanaka, Y., Bannai, E., Kawai, S., and Yamane, T., *J. Cryst. Growth*, 1975, vol. 30, pp. 193–197.
- Liu, X., Zhao, L., Hou, W., Wenhui Su, W., *Sci. China, Ser. B*, 1994, vol. 3, pp. 1054–1060.
- Otani, S., Nakagawa, H., Nishi, Y., and Kaieda, N., *J. Solid State Chem.*, 2000, vol. 154, pp. 238–241.
- Blazevic, N., Kolbah, D., Belin, B., Sunjic, V., and Kajfez, F., *Synthesis*, 1979, vol. 14, p. 161.
- Subramania, A., Angayarkanni, N., and Vasudevan, T., *Mater. Chem. Phys.*, 2007, vol. 102, pp. 19–23.
- Wang, J., Wang, Y., Qiao, M., Xie, S., and Fan, K., *Mater. Lett.*, 2007, vol. 61, pp. 5074–5077.
- Weinzierl, D., Touraud, D., Lecker, A., Pfitzner, A., and Kunz, W., *Mater. Res. Bull.*, 2008, vol. 43, pp. 62–67.
- Leunga, Y.H., Djuris, A.B., Liua, Z.T., Lia, D., Xiea, M.H., and Chan, W.K., *J. Phys. Chem. Solids*, 2008, vol. 69, pp. 353–357.
- Prakash, A.S., Khadar, A.M.A., Patil, K.C., and Hedge, M.S., *J. Mater. Synth. Process.*, 2002, vols. 3, 10, pp. 135–141.
- Chouziera, S., Afanasiev, P., Vrinata, M., Cserib, T., and Roy-Auberger, M., *J. Solid State Chem.*, 2006, vol. 179, pp. 3314–3332.
- Wang, H., Li, W., and Zhang, M., *Chem. Mater.*, 2005, vol. 17, p. 3262.
- Wang, H.-M., Wang, X.-H., Zhang, M.-H., Du, X.-Y., Li, W., and Tao, K.-Y., *Chem. Mater.*, 2007, vol. 19, p. 1801.
- Wang, H., Du, X., Zhang, M.-H., Li, W., and Tao, K.-Y., *Catalysis Today*, 2008, vol. 131, pp. 156–161.
- Afanasiev, P., *Inorg. Chem.*, 2002, vol. 41, p. 5317.
- Heymann, G., *Doctoral (Chem.) Dissertation*, Fakultät für Chemie und Pharmazie, Ludwig-Maximilians-Universität, München, 2007, pp. 69–70.